

## P-36: Effect of Stress of MgO protecting layer on Discharge Characteristics of AC-PDP

**Mi Jung Lee, Sun Young Park, Soo Gil Kim, Hyeong Joon Kim<sup>1</sup>**

School of Materials Science and Engineering, Seoul National University, Korea

**Sung Hwan Moon**

School of Materials Science and Engineering, Seoul National University, Korea

Samsung SDI Corporate R&D Center, 418-5 Gongse-ri, Kiheung-Eup, Yongin, Gyeonggi Province, Korea

**Jong Kuk Kim**

Korea Institute of Machinery & Materials, 66 Sangnam-dong, Changwon, Kyungnam, Korea

### Abstract

*The stress of MgO thin film, which is used as a dielectric protective layer in AC-PDP, was measured by a laser scanning method. MgO films were deposited by e-beam evaporation on glass substrates with dielectrics layer on them in various deposition temperatures ranging from room temperature to 300 °C. The compressive stress of MgO films was increased with increasing substrate temperature due to intrinsic stress accumulation, causing the densification of the films. Both firing voltage ( $V_f$ ) and sustaining voltage ( $V_s$ ) were reduced for the higher compressively stressed and densified films. In the other hand, another film properties such as preferred crystallographic orientation and surface roughness seemed not to influence the discharge characteristics of  $V_f$  and  $V_s$  significantly.*

### 1. Introduction

MgO protective layer reduce the discharge voltage of PDPs due to its high secondary electron emission coefficient ( $\gamma_i$ ), resulting in less energy consumption [1]. The improvement in the discharge characteristic of MgO protective layers is the essential research topic in the fabrication of PDPs. However, what property of MgO affects dominantly the discharging properties of PDPs has not been exactly known. Various physical and chemical properties of MgO film, such as surface roughness, density, and stoichiometry, have been suggested as a key factor to govern the discharge characteristics. But up to now no reasonable results, which can give a complete explanation for it, have been reported [2-4].

The stress in thin film is known to have much correlation not only with the physical properties of films like mechanical strength related to failure of materials, but also with electrical properties such as dielectric constant, resistivity, and carrier mobility [5,6]. The stress of MgO film in AC-PDP has been investigated only in view of mechanical properties like crack propagation [7]. However, it has not been reported yet the influence of the stress of MgO films on the electrical properties

in AC-PDP like lowering the operating voltage. Therefore, the relationship between the discharge characteristic and the residual stress of MgO thin film has been studied in this work. The laser scanning method was used to measure the stress of MgO film. And the relation with other properties of films was also evaluated by x-ray diffraction (XRD), atomic force microscopy (AFM), and scanning electron microscopy (SEM). Film density was also measured using a gravimetric method. Finally, the firing voltage ( $V_f$ ) and sustaining voltage ( $V_s$ ) were characterized to find out the relationship between the discharging and the MgO properties.

### 2. Experiments

MgO thin films were deposited on a glass substrate with a dielectric layer on it by e-beam evaporation method in a vacuum chamber of  $5 \times 10^{-7}$  Torr. MgO single crystal pellets ( $3 \times 3 \text{ mm}^2$ , 99.99 % purity) were used as a source and no gas was flown during deposition. Substrate temperature was varied from room temperature to 300 °C. The deposition rate was kept at 0.3 nm/s and the final MgO film thickness was 500 nm for all samples. The film structure and preferred crystallographic orientation was characterized by XRD in  $\theta$ - $2\theta$  mode. RMS roughness and average roughness were measured by AFM. The film density was obtained by dividing the measured weight by measured volume. All the samples were carefully treated not to be exposed to air and water, because MgO is known to have a strong hydration inclination. Laser scanning method was used to determine the film stress by measuring the curvature change of substrate. Initial curvature of a glass substrate was measured before deposition and compared with the curvature after deposition. In this method, Stoney's equation is used to calculate the film stress;

$$\sigma_f = \left( \frac{E_s}{1-\nu_s} \right) \frac{t_s^2}{6t_f} \Delta K = \left( \frac{E_s}{1-\nu_s} \right) \frac{t_s^2}{6t_f} \left( \frac{1}{R_i} - \frac{1}{R_f} \right)$$

where  $E_s$  is the Young's modulus of glass substrate,  $\nu_s$  the Poisson's ratio of substrate,  $t_s$  and  $t_f$  thickness of substrate and film, respectively. And  $R_i$  and  $R_f$  are the curvature of substrate

<sup>1</sup>.TEL: +82-2-880-7378, e-mail: hjkim@plaza.snu.ac.kr

before and after deposition. This method determines the film stress according not only to the film properties but also to substrate elastic properties. The Young's modulus  $E_s$  and Poisson's ratio  $\nu_s$  were assumed to be 76.5 GPa and 0.21, respectively.

Firing voltage ( $V_f$ ) and sustaining voltage ( $V_s$ ) were also measured with a unsealed 2" panel, which was discharged in the chamber filled with Xe (4 %)-Ne gas at 400 Torr. The front panel with MgO layer was just put over the rear panel with a phosphor layer. This system can exclude the variation of rear panel quality by using the same rear panel. 10 kHz sustaining pulse was applied.

### 3. Results and Discussion

MgO films on glass substrate had compressive stress regardless of deposition temperature, as shown in Figure 1, which also shows that the stress increased with substrate temperature. The stress of film consists of the intrinsic and extrinsic stresses. Extrinsic stress is known as a thermal stress. Thermal stress is caused by the difference in thermal expansion coefficient of substrate and film.

$$\sigma_{thermal} = M \cdot (\alpha_f - \alpha_s) \cdot (T_d - T_m)$$

where  $M$  is the biaxial modulus of thin film, and  $\alpha_f$  and  $\alpha_s$  the thermal expansion coefficients of film and substrate, respectively.  $T_d$  and  $T_m$  represent the deposition temperature and measuring temperature, respectively. MgO had higher thermal expansion coefficient,  $13.6 \times 10^{-6} \text{ }^\circ\text{C}^{-1}$ , compared to that of glass substrate,  $8.3 \times 10^{-6} \text{ }^\circ\text{C}^{-1}$ . In case of deposition at  $300 \text{ }^\circ\text{C}$  and measuring the stress at room temperature, the thermal stress developed in films should be a positive tensile stress. Even though the biaxial modulus  $M$  is varied with a phase or orientation in the same materials, MgO film biaxial modulus with a order of GPa can be assumed considering that bulk MgO has about 300 GPa of Young's modulus [8]. Consequently, MgO film deposited at elevated temperature should have a tensile thermal stress at least in the range of several hundreds MPa, and increase as the deposition temperature elevates.

But Figure 1 shows that the stresses of film changed toward more compressive stress in higher deposition temperature. This opposite tendency looks quite strange. The other stress beside thermal stress, intrinsic stress, seems to be a cause for this. The sample deposited at room temperature can be regarded as having no thermal stress because  $T_d - T_m$  is zero. Thus the compressive stress developed in the sample deposited in room temperature might be originated from intrinsic stress.

Though the intrinsic stress generally tends to be reduced when MgO film is deposited in elevated temperature, the factors and mechanism forming an intrinsic stress have not been known exactly yet. In this work, intrinsic stress of MgO film increased largely toward compressive stress in higher substrate temperature with compensating the higher thermal tensile stress. The strong compressive intrinsic stress formed during film formation influenced on the microstructure of MgO film and it will be discussed in detail in the following paragraph. Firing voltage and sustaining voltage measured in a real panel with MgO protective layer are shown in Figure 2. Firing voltage decreased as the temperature increased. The sustaining voltage also decreased even though the slope was not as much as that of the firing voltage. It can be noticed that the discharge voltage is lower in the highly compressed sample. To examine the relation of these two properties, film stress and discharging voltage, other properties of MgO film were also investigated. Surface roughness is measured by atomic force measurement (AFM). Rms roughness and average roughness change in the range of

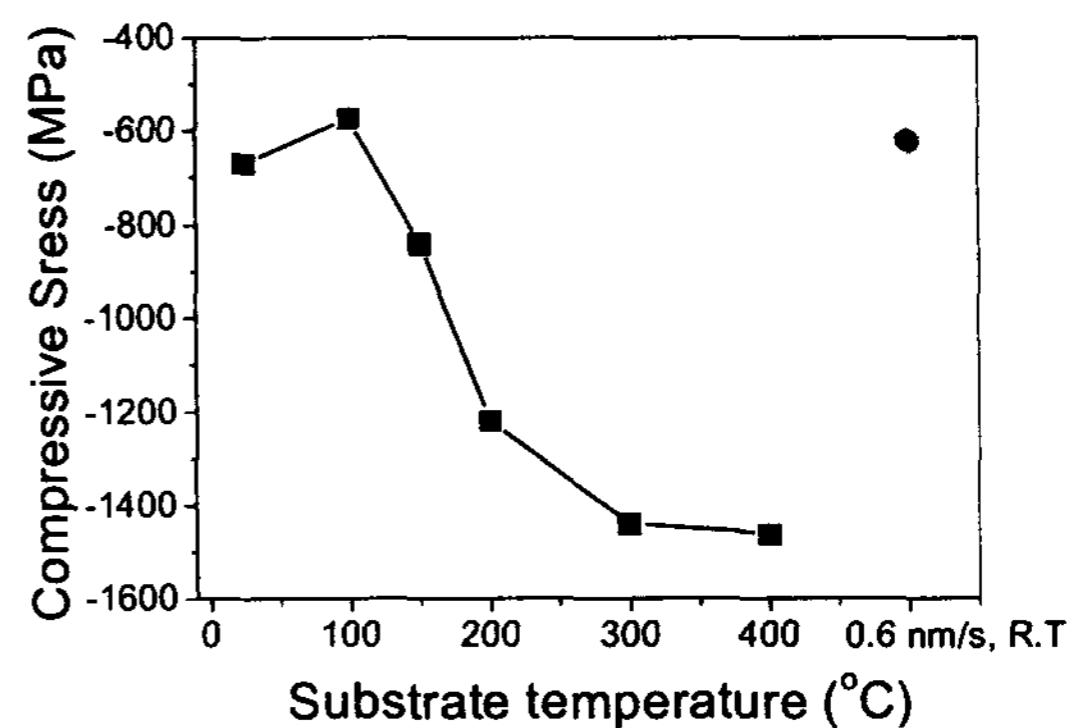


Figure 1. Stresses of MgO films with substrate temperature variation.

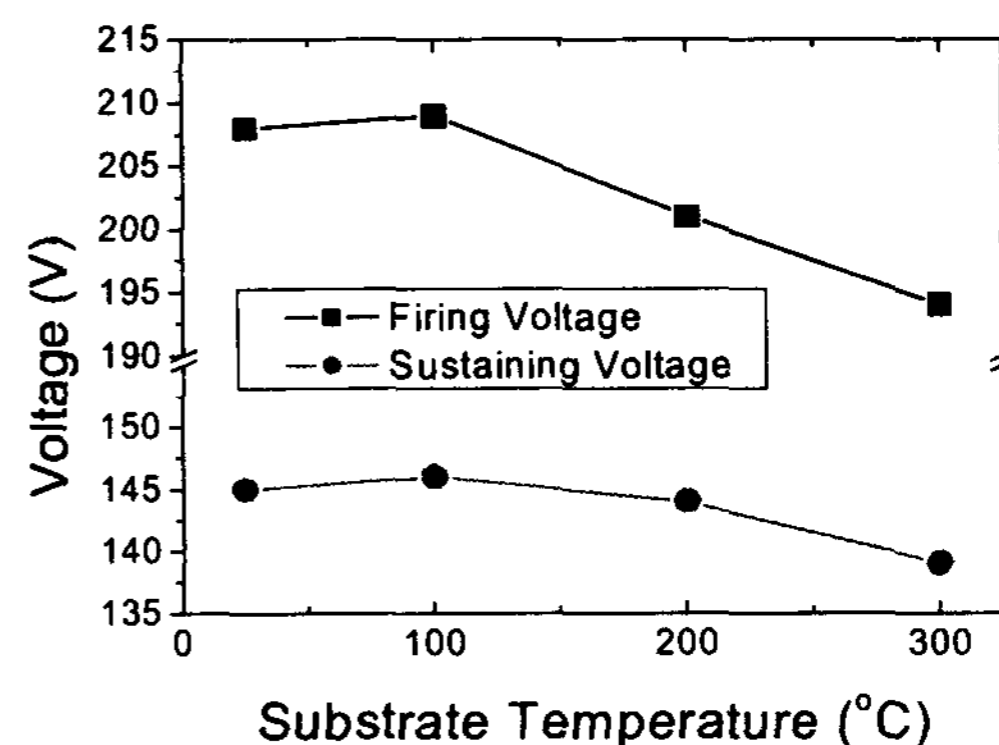


Figure 2. Firing voltage and sustaining voltage with substrate temperature in real panel.

about 2.7~3.7 nm and 2.1~2.9 nm, respectively, with the substrate temperature. Any noteworthy tendency could not be found in the result. The correlation between two properties was not found in this work. Preferred crystallographic orientation analyzed by XRD in  $\theta$ - $2\theta$  mode is shown in Figure 3. MgO film had (200) preferred orientation at low deposition temperature, but (111) peak became stronger and (220) peak began to appear above  $200 \text{ }^\circ\text{C}$ . The orientation and film stress seems to have a strong correlation; (111) peak increased while (200) peak decreased as the compressive stress increased. The relationship between the secondary electron emission coefficient,  $\gamma_i$ , which determines the discharge properties of MgO, and crystallographic orientation are not clear yet. Film orientation is one of the concerning factors. However, a reported result, in which orientation is more profitable to lower the discharge voltage, is not consistent with another [9-11].

We prepared another samples to find out the relation between film orientation and discharging properties. Peak intensity of each sample is shown in Figure 4. The sample deposited in 0.6 nm/s was compared with the  $200 \text{ }^\circ\text{C}$  sample, because they had almost the same crystallographic orientation, as shown in Figure 4. Stress of comparison sample deposited in 0.6 nm/s was -622 MPa, and was certainly distinguished from stress, -1220 MPa, of film deposited at  $200 \text{ }^\circ\text{C}$  in 0.6 nm/s. The firing voltage and sustaining voltage were 212 V and 149 V, respectively. These

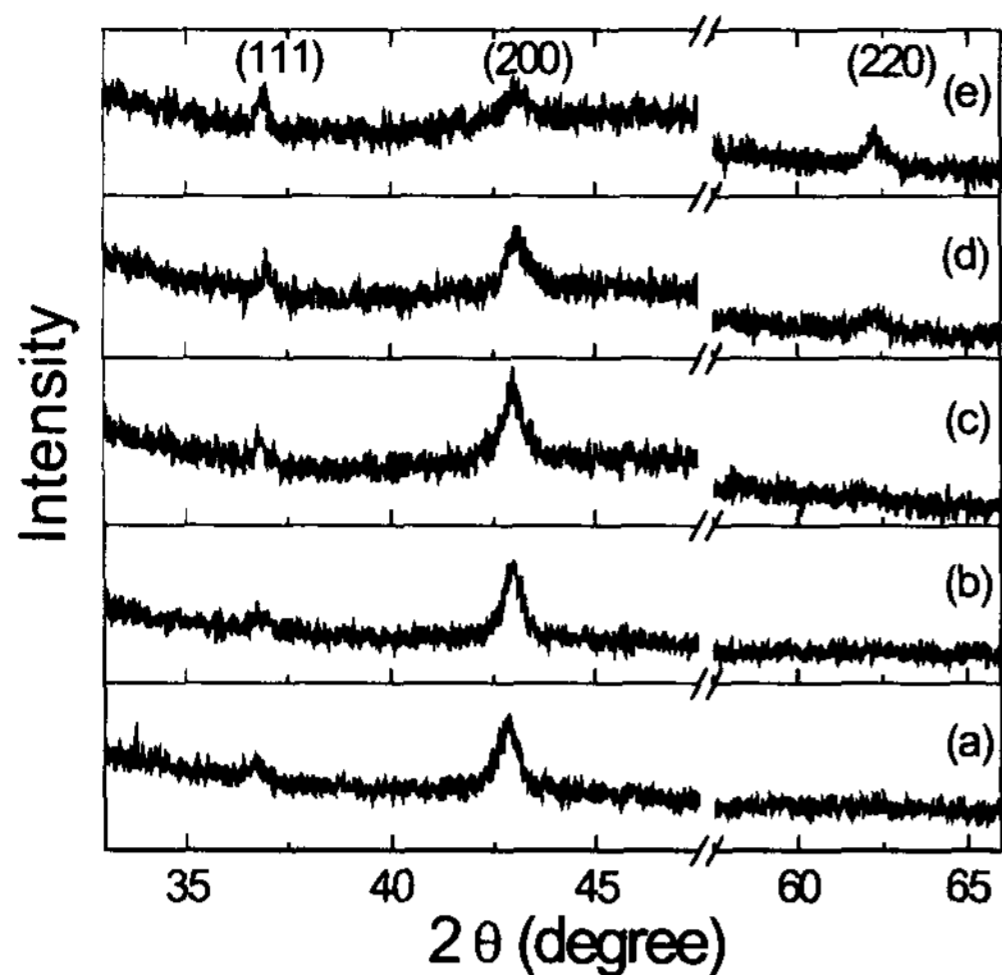


Figure 3. XRD analysis MgO films in various deposition temperature. (a) room temperature, (b) 100 °C, (c) 150 °C, (d) 200 °C, and (e) 300 °C.

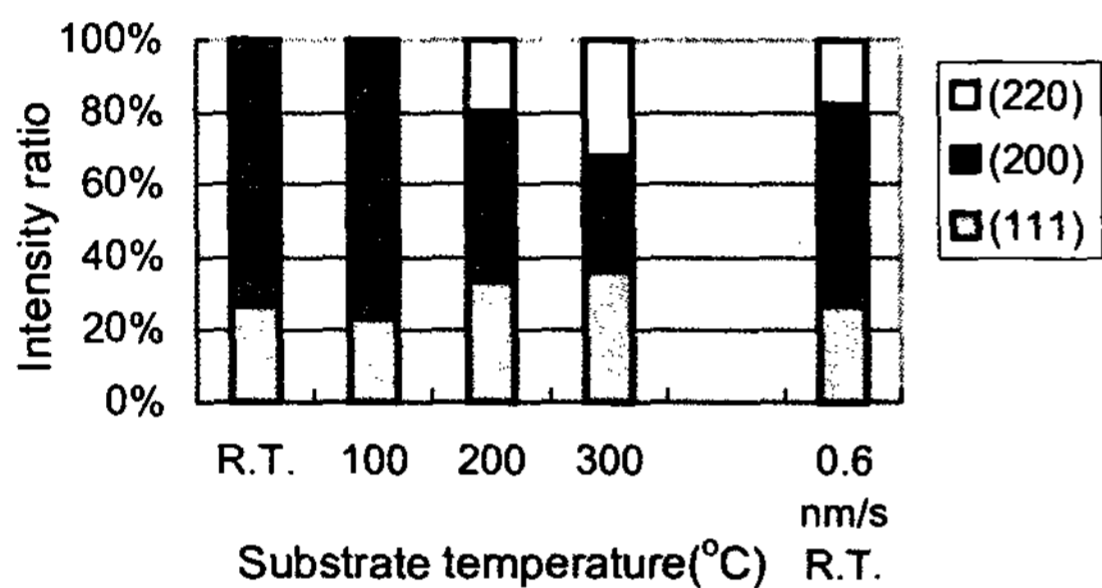


Figure 4. XRD peak ratio of films deposited at various temperature and comparative sample with different deposition rate.

properties are rather similar to those of low deposition temperature films than those of deposited at 200 °C. So, the preferred orientation can be excluded from the factors to influence film stress and discharge characteristic. At the same time, this result can provide an indirect evidence for the correlation between film stress and discharging property.

The plan-view and cross-sectional SEM micrographs of MgO films are shown in Figure 5 and 6. In Figure 5 (a) and (b), porous structure with open grain boundary was seen in the film deposited at lower temperature, while massed structure with closed grain boundary in film deposited at higher temperatures in Figure 5 (c) and (d). Reminding that dramatic increase of the compressive stress in film deposited above 100 °C, these structures are supposed to have strong relation with the film stress. Cross sectional images in Figure 6 also support this relation, too. Tilted and unshaped structure appeared in the cross-sectional image of the room temperature deposited film. In the film deposited at 100 °C, the splitted small grains with loose grain boundaries existed. In the deposition temperature above 200 °C, the columnar structure having perpendicular direction to the substrate begins to appear shown in Figure 6 (c). Finally, the clearly shaped columns through thickness are shown

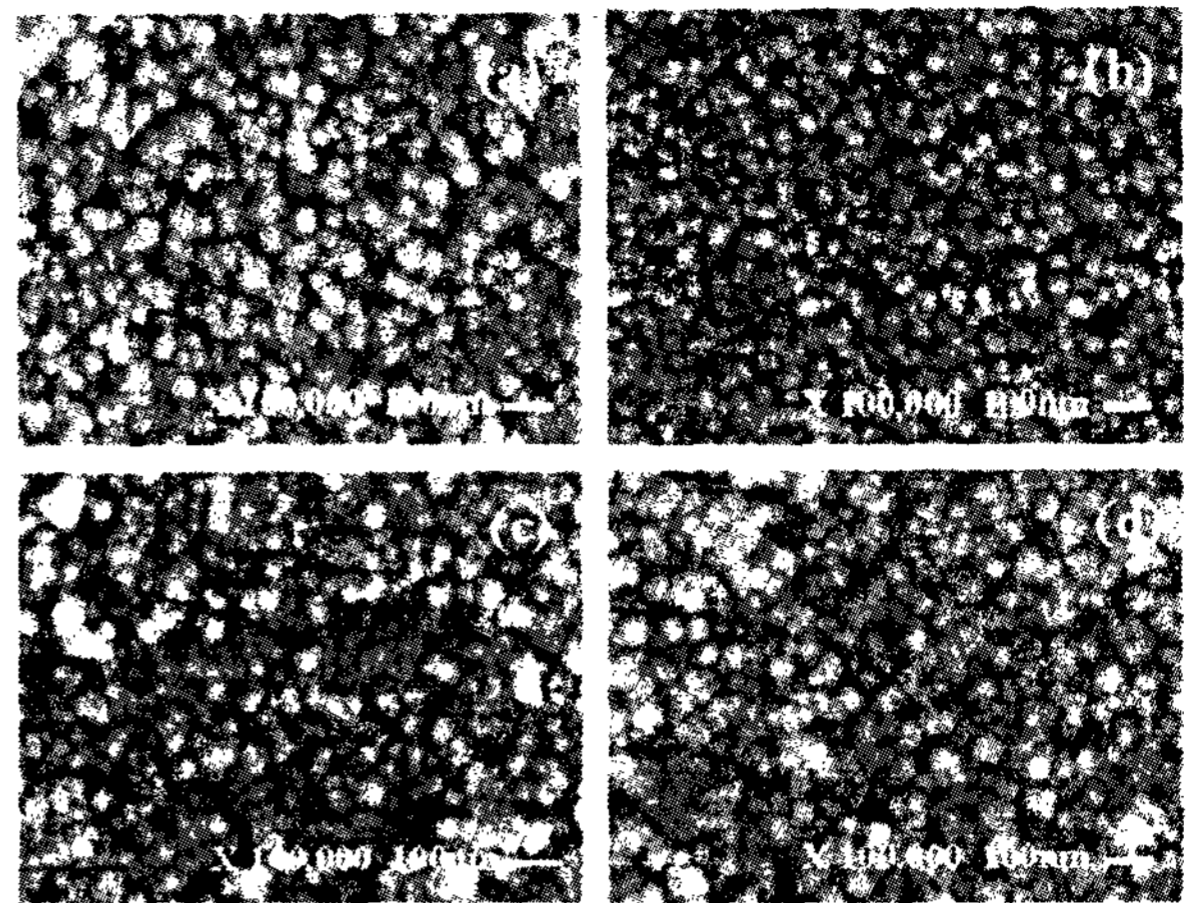


Figure 5. SEM plane image of MgO film deposited (a) at room temperature, (b) 100 °C, (c) 200 °C, and (d) 300 °C.

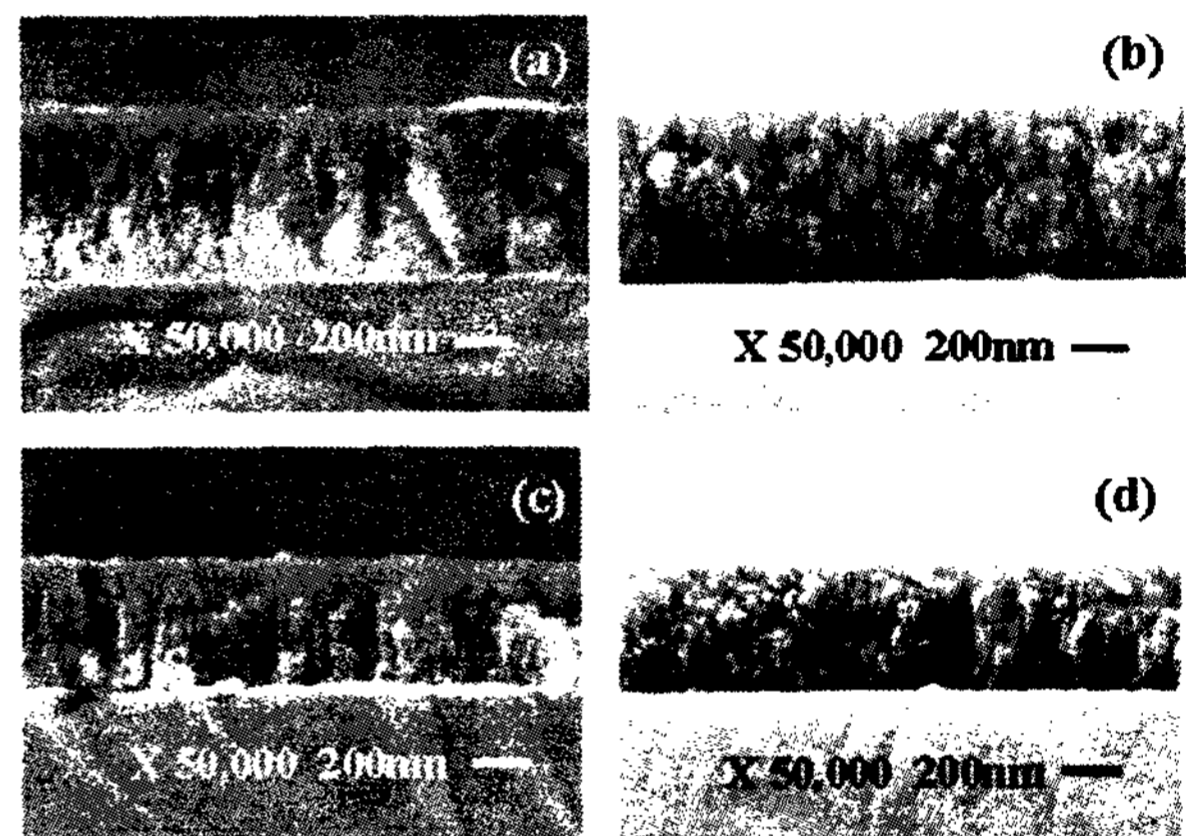
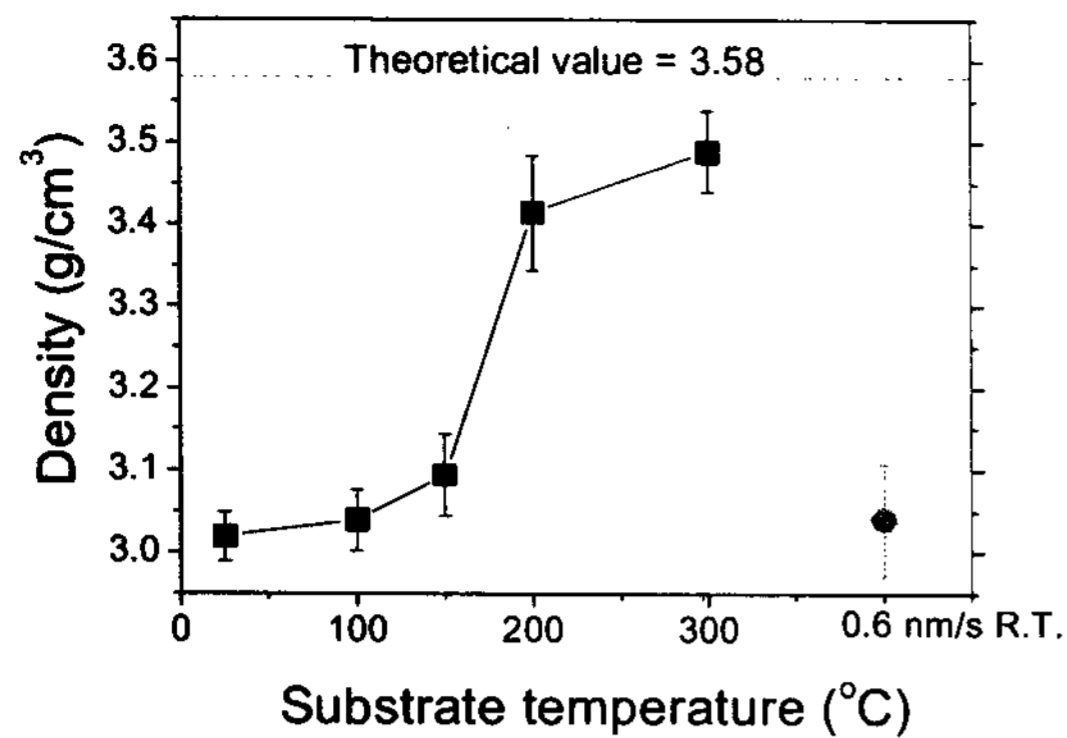


Figure 6. SEM cross sectional image of MgO film deposited (a) at room temperature, (b) 100 °C, (c) 200 °C, and (d) 300 °C.

for the films deposited at 300 °C, as shown in Figure 6 (d). Because MgO is a refractory oxide with high melting point, 2800 °C,  $T_d/T_m$  is a small value even for the highest substrate temperature in this experiment.  $T_d$  is the deposition temperature and  $T_m$  is the melting temperature. So, elliptical grains with a width larger than film thickness are hardly expected. Figure 6 (a) is pertinent to the zone 1, Figure 6 (b) and (c) are to zone T and the onset of the zone 2 structure begins to appear in Figure 6 (d), according to the zone model of Hentzell for evaporated films [12]. Transition of microstructure from the zone 1, to the zone T and the zone 2 decreases porosity and makes dense films. Figure 7 is the quantified density of the MgO film by the gravimetric method. To measure the density of film by refractive index exactly in multiplayer structure, glass and dielectric layer, is very complex process. Thus the gravimetric method based on the Archimedes' principle was used. The tendency of film density was quite coincident well with stress of film. It is worthy of attention that a drastic increase in density between 100 °C and 200 °C is congruous with a large increase in the stress in same range. This distinguishable difference above 100 °C was also observed in SEM image analysis. In addition, the comparative sample deposited in 0.6 nm/s, which had relatively low compressive stress similar to the low deposition temperature samples, had low density. Its discharging voltage



**Figure 7. Density of films measured by gravimetric method.**

was within the tendency of the stress and density.

In view of the results obtained so far, higher compressive stress of film formed during deposition makes the MgO film denser. Many materials properties in bulk are varied in thin film and it is caused by its basic microstructure, which are closely related each other. The most conspicuous properties of thin film state against bulk state is large amount of defect, which includes grain boundaries, pores and sparse structure. Higher film density means small grain boundary region and low defects, which approaches to bulk properties. The better properties of MgO film to lower the discharge voltage in AC-PDP are expected in the solid microstructure. This can be obtained by the highly compressed dense film. To make sure of it, the comparison and analysis of bulk state and thin film state MgO would be studied further.

#### 4. Conclusion

MgO films were deposited in various substrate temperature and measured their stress and other properties to clear which factors affect the discharge characteristics of MgO film in AC-PDP. Compressive stress of the MgO film increased as deposition temperature increased and highly compressed film showed better discharge properties, lower firing and sustaining voltage. Surface roughness measured in each sample by AFM did not changed noticeably. Preferred crystallographic orientation of MgO film surely changed with film stress, but the additional sample deposited in 0.6 nm/s which had the same orientation to the 200°C deposited sample had definitely different film stress

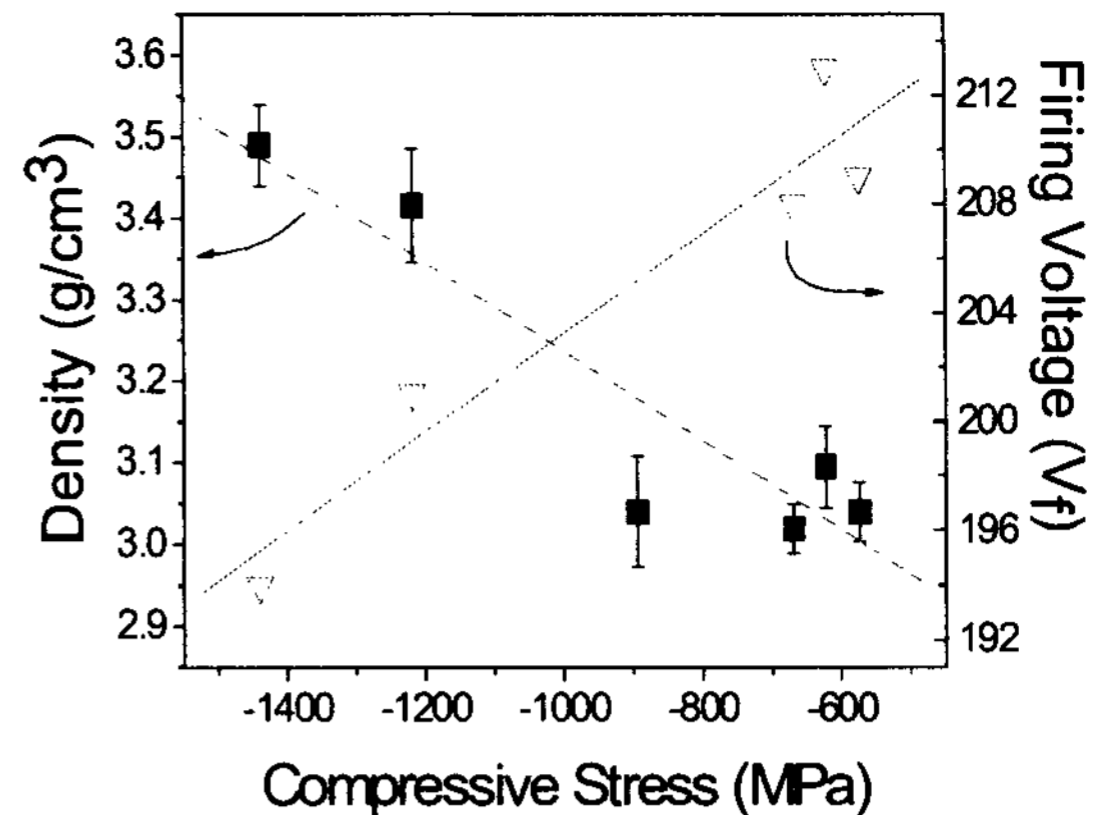


**Figure 8. Correlation of film stress, density and discharging properties**

and discharge property from those of the 200°C deposited sample. Microstructure and density were strongly related to film stress, and it can be confirmed by SEM micrograph and quantified density. Better discharging characteristic could be obtained in the highly compressed denser MgO film.

#### 5. Acknowledgements

We would like to appreciate the financial assistance of Ministry of Information and Communication of Korea by IMT 2000 project.

#### 6. Reference

- [1] H. Uchiike *et al*, IEEE Trans. Elec. Dev., ED-23 1211 (1976).
- [2] H. K. Hwang. *et al*, Surf. and Coat. Tech., **177-178**, 705 (2004).
- [3] J. K. Kim *et al*, J. Vac. Sci. and Tech. B, **19** (3),687 (2001).
- [4] Ch. Heyn *et al*, J. Cry. Growth, **251** (1-4), 231 (2003).
- [5] W. Y. Park *et al*, Appl. Phy. Lett., **83** (21), 4387 (2003).
- [6] An, Steegen, Mater. Sci. and Eng.: R., **38** (1),1 (2002).
- [7] S. BaBa *et al*, Thin Sol. Films **164**, 169 (1988).
- [8] M. A. Meyers *et al*, Mechanical Behavior of Materials, Prentice Hall, 92 (1999).
- [9] E. H. Choi *et al*, Jpn. J. Appl. Phys. **41**, L1006 (2002).
- [10] Y. H. Cheng *et al*, J. Appl. Phys., **93** (5), 1422 (2003).
- [11] A. Boughariou *et al*, J. Appl. Phys., **95** (8), 4117 (2004).
- [12] H. T. G. Hentzell *et al*, J. Vac. Sci. Tech. A, **2**, 218 (1984).